Supplementary METHODS

***Stab2*-Cre mouse.** A BAC encoding the genomic *Stab2* locus (RPCIB731O23129Q) was obtained from SourceBioscience. A cDNA containing a codon improved version of cre recombinase (1) followed by polyA signal sequence was fused into exon 1 of *Stab2* via homologous recombination (2). In frame recombination into *Stab2* was realized via PCR added homologous arms of 45 bp in length flanking the 5' and 3' region of the start codon. Correct *Stab2*-cre recombinant BAC was linearized, purified with Sepharose CL4B (GE Life Science), and injected into the pronuclei of fertilized C57Bl/6NCRL oocytes. Three B6.Stab2$^{tg1.1\text{-}3cre}$ transgenic founder mice were identified by PCR and further characterized by crossing to stop floxed R26LacZ [B6.129S4-Gt(ROSA)26Sor^{tm1Sor}; JAX#003474] (3) and R26YFP [B6.129X1-Gt(ROSA)26Sor$^{tm1(EYFP)Cos/}$J; [JAX 006148] (4) reporter animals. The founder B6.Stab2$^{tg1.2cre}$ displayed Cre activity in liver sinusoidal endothelial cells (LSEC) according to native Stabilin-2 expression and was used in this study as *Stab2*-Cre line. *Lyve1*-Cre [B6.129P2-*Lyve1*$^{tm1.1(EGFP/cre)Cys/}$J; JAX#012601]) (5) was used as mouse line offering Cre expression in LSEC and lymphatic EC.

Generation of conditional knockout mice. *Stab2-Cre* mice were crossed to mouse lines bearing floxed alleles of *Gata4* (B6;129-*Gata4*$^{tm1.1Sad/}$J; Jax#008194] (6), *Bmp2* [B6;129S4-*Bmp2*$^{tm1Jfm/}$J; Jax#016230] (7), *Rspo3* [B6-Rspo3$^{tm1.1Arte}$; TaconicArtemis] (8) (kind gift of C. Niehrs/U. Fenger, Deutsches Krebsforschungszentrum, DKFZ, Heidelberg, Germany), *Wls* [B6-Gpr177$^{tm1\ 1775.302Arte}$; TaconicArtemis] (9) (kind gift of M. Boutros/I. Augustin, Deutsches Krebsforschungszentrum, DKFZ, Heidelberg, Germany), and *Hgf* [B6;129-*Hgf*^{tm1Jmw}/Mmnc; MMRRC:000423] (10). The mouse strain B6;129-*Hgf*$^{tm1Jmw/}$Mmnc, identification number 423-UNC, was obtained from the Mutant Mouse Regional Resource Center, a NIH funded strain repository, and was donated to the MMRRC by Steven E. Raper, Ph.D., University of Pennsylvania Medical Center. To obtain loss-of-function and control genotypes *Stab2*-Cre$^{tg/wt}$;*Gata4*$^{fl/wt}$ (*Stab2*-Cre$^{tg/wt}$;*Hgf*$^{fl/wt}$, *Stab2*-Cre$^{tg/wt}$;*Rspo3*$^{fl/wt}$, *Stab2*-Cre$^{tg/wt}$;*Wls*$^{fl/wt}$, and *Stab2*-Cre$^{tg/wt}$;*Bmp2*$^{fl/wt}$, respectively) were crossed to *Gata4*$^{fl/fl}$ (*Hgf*$^{fl/fl}$, *Rspo3*$^{fl/fl}$, *Wls*$^{fl/fl}$, and *Bmp2*$^{fl/fl}$, respectively) mice. The *Lyve1*-Cre mouse strain was crossed to floxed *Gata4,* R26LacZ and R26YFP animals as described for *Stab2*-Cre mice.

Quantification of endothelial Gata4 knockdown in *Stab2*-Cre;*Gata4*$^{fl/fl}$ fetal liver. *Stab2*-Cre;*Gata4*$^{fl/fl}$ and control embryos at E11.5 were co-stained with GATA4, Toto-3, CD31 and LYVE1 (the same secondary antibody was used for CD31 and LYVE1 in order to detect both, LSEC (LYVE1$^+$) as well as capillarized EC (CD31$^+$)). The number of GATA4$^+$ EC (CD31$^+$ and/or LYVE1$^+$) was counted using the ImageJ software (NIH) cell counter and quantified as number of GATA4$^+$ EC per 1 mm² of fetal liver area.

Transplantation. Fetal livers from E13.25 *Stab2*-Cre;*Gata4*$^{fl/fl}$ and control embryos were mechanically dissociated and passed through a 100 µm cell strainer (BD). After incubation with purified mouse IgG (500 µg/ml, Jackson ImmunoResearch Laboratories) in 5% FCS/PBS the cells were stained with commercial antibodies in 5% FCS/PBS on ice for 30 min. Lineage-negative Sca-1$^+$ Kit$^+$ (LSK) (number of sorted cells ranged between 150 and 850 cells) were isolated by electronic deposition into individual wells of a U-bottom 96-well plate containing 100 µl sterile 50% FCS using a FACS AriaIII (BD). Prior to injection, 100 µl sterile PBS was added to each well, and cells were injected intravenously into individual Rag2$^{-/-}$;$\gamma_c^{-/-}$;Kit$^{W/Wv}$ recipients (11). Peripheral blood samples were collected 4, 10 and 15 weeks after transfer from the submandibular vein into EDTA-containing microtubes (Sarstedt) to screen for progeny of donor cells (detected by the congenic marker CD45.1).

Red blood cell lysis to enrich for white blood cells was performed by using RBC Lysis Buffer (Biolegend). For FACS staining, the following antibodies were used: CD3e eFluor780 (clone 17A2, # 47-0032-80, eBioscience), CD11b PE-Cy7 (clone M1/70, # 25-0112, eBioscience), CD45.2 PE (clone 104, #12-0454, eBioscience), CD45.1-FITC (clone A20-1.7, #561871, BD), Gr-1 APC (RB6-8C5, # 553129, BD), CD19 QDot605 (clone 6D9, #Q10379, Invitrogen). To assess the recombination of the *Gata4* locus in the peripheral blood cells of transplanted animals, DNA was purified from the blood using a DNeasy Blood&Tissue Kit (Qiagen) and PCR analysed (5'-aacctgagcagctgatgact-3' and 5'-ctagactattgatcccggagtg-3). A 400bp PCR product was detected in gel electrophoresis upon loss of *Gata4* exons 3 to 5.

Animal handling. All animal experiments were approved by the animal ethics committee in Baden-Wuerttemberg (Regierungspraesidium Karlsruhe).

Embryo dissection, cryopreservation, and paraffin embedding. Pregnant mice were sacrificed by cervical dislocation. Embryos were dissected and the yolk sac was collected for genotyping. Photomicrographs and videos were generated with a DMIL stereomicroscope (Leica). Embryos were either embedded in OCT compound (Sakura) and frozen in liquid nitrogen or fixed in 4% PFA at 4°C, followed by paraffin embedding according to routine protocols. For GFP/YFP staining embryos were embedded in OCT after incubation over night in 4% PFA followed by 24 h 30% sucrose treatment.

Primary endothelial cells. Rat LSEC [rLSEC] and lung microvascular EC [rLMEC] were isolated, purified and cultured as previously described (12). Murine LSEC [mLSEC] were isolated and purified using CD146 (LSEC) MicroBeads as previously described by Diehl et al. (13) and were cultured at 37°C and 5% CO_2 for the indicated time intervals on culture plates pre-coated with Collagen IV (Sigma) in DMEM containing 10% FCS, 1% penicillin/streptomycin, and 2% L-Glutamine (all Biochrom). Purity of murine LSEC was confirmed by FACS with directly-labelled antibodies against Stabilin-2 and CD11b. HUVEC, HDLEC and HUASMC (all PromoCell), HLSEC (ScienCell Research), bEnd5 and bEnd3 (both ATCC) were grown in culture media as recommended by the suppliers.

Adhesion model. 96-well plates were coated either with 0.15 mg/ml Collagen IV (Sigma), 0.01 mg/ml LN-211, or LN-411 (Biolamina) at 4°C (overnight) and blocked with 1% BSA at 37°C for 1 h. LX - 2 cells (generous gift from Scott Friedman, New York) growing at 37°C and 5% CO_2 in DMEM containing 2% FCS and 1% P/S were detached with cell dissociation buffer (Life Technologies) and incubated at 37°C for 2-3 h on a falcon tube roller to prevent adhesion. 50,000 cells were seeded in triplicates on adhesive 96-well plates in serum-free DMEM, incubated 30 min at RT followed by 80 min at 37°C. After washing, adherent cells were stained with crystal violet solution and measured at 570 nm with an Infinite 200 Pro reader (Tecan). For analysis with the real time cell analyzer xCelligence system (Roche) 10,000 cells were seeded in triplicates on coated E-Plate 16 (ACEA Bioscience) in serum-free DMEM, incubated 30 min at room temperature followed by 24 h at 37°C. Electrical impedance of each well was measured every 15 seconds and converted into the cell index by a computer based algorithm. The increase of the cell index over time (slope) was calculated by the xCelligence Software and used as quantitative indicator of adhesion.

Retroviral transduction of EC. Human *GATA4* cDNA (IMAGE:8144111) was cloned into pBabePuro vector (Addgene). To obtain recombinant retroviral particles, Phoenix producer cells [ATCC CRL-3213] were lipofected with vector DNA as described (14). Filtered

supernatants were applied to target cells at three consecutive days. Before harvesting (day 7) puromycin (Invitrogen) was added (day 5) at a concentration of 1 µg/ml.

Lentiviral transduction of EC. Synthetic codon optimized cDNA (GeneArt) referring to murine *Gata4* (GenBank: AB075549.1) amino acid sequence was cloned in combination with IRES, mCherry, T2A, and puromycin into pLenti-EF1α vector (15). To obtain m*Gata4*-IRES-mCherry-puromycin and control (IRES-mCherry-puromycin only) expressing lentiviral particles HEK293T cells were co-transfected with vector DNA, pMD2.G L1 (Addgene), pMDLg/pRRE L3 (Addgene), and pRSV rev L2 (Addgene) plasmids using X-tremeGENE 9 (Roche) transfection reagent as described (16). Conditioned supernatants were harvested 48 h, 60 h and 72 h after transfection, filtered (0.45 µm, Carl Roth) and concentrated using Vivaspin 20 MWCO 100000 columns (Sartorius). Concentrated supernatants were applied to bEnd3 cells. Selection was carried out with 2 µg/ml Puromycin (Invivogen) and transfection efficiency was visualized by red fluorescence.

Quantitative reverse-transcription PCR (qRT-PCR). Primers were designed using Primer-Blast (NCBI) and are available upon request. Total RNA extracted with EZNA^{TM} Total-RNA-Kit (OMEGA Biotec) was reverse transcribed into cDNA with RevertAid H-Minus M-MuLV transcriptase (ThermoScientific). QRT-PCR was performed in Mx3005P system (Stratagene) using SYBR Green PCR Master-Mix (Applied Biosystems) as described (12). Relative gene expression in relation to reference gene (*β-Actin*) was calculated with MxPro Software (Agilent Technologies).

Microarray processing and statistical analysis. Gene expression profiling was performed using arrays Mogene-2.0-st, and HG-U133 Plus 2.0-st from Affymetrix. cDNA and cRNA synthesis and hybridisation to arrays were performed according to the recommendations of the manufacturer. A custom CDF Version14 (HG-U133 Plus 2.0), and Version18 (Mogene-2.0-st) with Entrez based gene definitions was used to annotate the arrays. The raw fluorescence intensity values were normalised applying quantile normalisation. Differential gene expression was analysed with the ANOVA, using a commercial software package SAS JMP7 Genomics, version 6, from SAS (SAS Institute). A false positive rate of a = 0.05 with false discovery rate correction was taken as the level of significance. The raw and normalised data are deposited in the Gene Expression Omnibus database (http://www.ncbi.nlm.nih.gov/geo/; accession No. GSE20375 and GSE92357). A published list of genes with *Gata4* transcription factor binding of adult mouse liver identified by ChIP-seq analysis (GEO GSE49131) was aligned to differentially expressed genes of E11.5 mouse *Stab2*-Cre$^{tg/wt}$;*Gata4*$^{fl/wt}$ fetal liver.

Antibodies. Primary antibodies: rat anti-F4/80 (clone BM8, #123102, BioLegend), rat anti-CD11b-PE (clone M1/70, #553311, BD Pharmingen), rat anti-CD68 (clone FA-11, #137002, BioLegend), hamster anti-CD31 (clone 2H8, #MA3105, Thermo Fisher Scientific), rat anti-CD31 (clone MEC13.3, #102502, BioLegend), mouse anti-CD31 (clone JC70A, #IR610, Dako), polyclonal goat anti-CD32b (#AF1330 and #AF1460, R&D Systems), polyclonal rabbit anti-GATA4 (#sc-9053, Santa Cruz), polyclonal rabbit anti-β-actin (#A2103, Sigma), polyclonal goat anti-Clec1b (#AF1718, R&D Systems), polyclonal rabbit anti-PROX1 (#102-PA32, ReliaTech), Alexa Fluor 488 Phalloidin (#A12379, Life Technologies), mouse anti–Stabilin-2 clone 3.1 antibody (17), polyclonal rabbit anti-LYVE1 (#103-PA50S, ReliaTech), polyclonal goat anti-LYVE1 (#AF2125, R&D Systems), rat anti-Liv2 (clone Liv-2, #D118-3, MBL), polyclonal rabbit anti-cleaved Caspase-3 (clone 5A1E, #9664, Cell Signaling), polyclonal goat anti-Ki67 (#sc-7846, Santa Cruz), Toto-3 iodide (#T3604, Life Technologies),

rat anti-Endomucin (clone eBioV.7C7, #14-5851-82, eBioscience), polyclonal rabbit anti-Caveolin-1 (#sc-894, Santa Cruz), polyclonal goat anti-Laminin α4 (#AF3837, R&D Systems), polyclonal rabbit anti-Collagen 15a1 (Sanna-Maria Karppinen, Finland), polyclonal goat anti-VE-Cadherin (#AF1002, R&D Systems), polyclonal rabbit anti-Desmin (#Ab15200, Abcam), rat anti-Ter119 (clone TER-119, #550565, BD Pharmingen), rabbit anti-Collagen type I (#R1038, Acris), rabbit anti-Collagen type III alpha 1 chain (#R1040, Acris), polyclonal rabbit anti-Collagen IV (#GTX19808, Genetex), rat anti-Tenascin-C (clone MTn-12, #ab6346, Abcam), polyclonal rabbit anti-Caspase-3 (#9661S, Cell Signaling), polyclonal rabbit anti-GFP/YFP (#A11122, Molecular Probes), rat anti mouse CD146 (clone: ME-9F1, #130-101-866, Miltenyi Biotec), polyclonal goat anti-IFITM (#sc-34171, Santa Cruz), rabbit anti-Cathepsin K (#11239-1-AP, Proteintech), rat anti–cytokeratin 19 (clone TROMA-III was deposited to the Developmental Studies Hybridoma Bank by Kemler, R., MPI fuer Immunobiologie, Freiburg, Germany (DSHB Hybridoma Product TROMA-III)), polyclonal goat anti-DPPIV/CD26 (AF954, R&D systems), mouse anti-human β-Catenin (clone 14, #610153, BD), polyclonal rabbit anti-mouse p-β-Catenin (#sc-22192-R, Santa Cruz), polyclonal rabbit anti-α-Catenin (#C2081, Sigma), polyclonal rabbit anti-Cre (#257003, Synaptic systems). Secondary antibodies: appropriate HRP-, Alexa Fluor 488, Cy2, Cy3, Cy5-conjugated secondary antibodies and Alexa Fluor 488-conjugated streptavidin were purchased from Dianova (donkey anti-rabbit Cy2, #711-225-152; goat anti-rat Cy3, #112-165-044; donkey anti-goat Cy3, #705-165-147; donkey anti-rat Cy3, #712-165-153; bovine anti-goat Cy3, #805-165-180; donkey anti-mouse Cy3, #715-165-151; donkey anti-goat Cy5 #705-175-147; sheep anti-mouse Cy5, #515-175-072; donkey anti-rabbit Cy5, #711-175-152; donkey anti-mouse Cy5, #715-175-151; donkey anti-mouse Alexa Fluor 488, #715-485-150; bovine anti-goat Alexa Fluor 488, #805-485-180; donkey anti-mouse Alexa Fluor 488, #715-485-151; goat anti-mouse HRP, #115-035-166; mouse anti-goat HRP, #205-035-108), GE-Healthcare (donkey anti-rabbit HRP, #NA934), Life Technologies (Streptavidin labelled Alexa Fluor 488, #S11223) and Jackson Immunoresearch (donkey anti-rat Cy2, #712-225-153; goat anti-rat Cy5, #112-175-003; Streptavidin labelled HRP, #016-030-084).

Immunofluorescence. Paraffin sections (1 - 5 µm) were de-paraffinized and rehydrated according to routine protocols. Antigen retrieval was carried out with Epitope Retrieval solution (Novocastra) at either pH 6 or pH 9. Cells grown on fibronectin-coated coverslips were fixed with 4% PFA, permeabilised with 0.1% Triton X-100 and blocked with 10% Donkey Serum (all Sigma). Cryosections (8 µm) were fixed with acetone or 4% PFA, permeabilised with 0.1% Triton X-100, quenched with 50 mM NH_4Cl and blocked in 5% FCS. First antibody was incubated over night at 4°C or 3h at RT, secondary antibody was incubated 45 min at RT. Sections and coverslips were mounted (Dako) and photographed with ECLIPSE Ni-E microscope (Nikon). For the quantification of stained structures (vascular bed: LYVE1, Stabilin-2, CD31; Hepatoblasts: Liv2; Erythroblasts: Ter119) specimens of at least three controls and *Stab2*-Cre;*Gata4*$^{fl/fl}$ embryos were prepared simultaneously and imaged with identical settings. Images were quantitatively analysed using ImageJ (NIH) software. In detail, the liver was marked as region of interest (ROI) and colour thresholds of the indicated markers were set in relation to the hepatic area (= fluorescent area %).

Quantification of apoptotic, proliferating and Desmin-positive cells. The numbers of TUNEL-, cleaved Caspase3-, Ki67-, and Desmin-positive cells in Stab2-Cre;Gata4$^{fl/fl}$ and control embryos were counted using the ImageJ software (NIH) and quantified as cell numbers per 1mm² of fetal liver area.

Confocal microscopy. Double or triple fluorescent-labelled sections were analysed by a TCS SP2 or TCS SP5 MP laser scanning spectral confocal microscope (Leica). The excitation wavelengths were set at 488, 543 and 633 nm. The emission maxima at 518, 570 and 673 nm were detected to visualise Alexa Fluor 488, Alexa Fluor 647, Cy3 Cy5 conjugates and Toto-3 respectively. Images were acquired in a sequential mode and processed with Leica confocal software and ImageJ software (NIH).

Immunohistochemistry. Acetone fixed cryosections (8 µm) were stained as described (17) and photographed using a brightfield microscope (Nikon). For hematoxylin & eosin, periodic acid-Schiff (PAS), and Sirius red staining, formalin-fixed, paraffin-embedded samples were processed according to standard protocols.

Hypoxyprobe measurements. Oxygen supply to mouse embryos was visualised by Hypoxyprobe^{TM}-1. Pregnant mice were injected i.p. with 60 mg/kg Hypoxyprobe^{TM}-1. 45 minutes following injection, mice were sacrificed and embryos were prepared as described above for PFA-fixed, paraffin embedded sections. To detect tissue hypoxia, 2 µm sections were stained with a monoclonal anti-pimonidazole antibody (clone 4.3.11.3) according to manufactures protocol.

β-galactosidase staining. For whole mount β-galactosidase staining, *Stab2*-Cre;R26LacZ embryos were rinsed in 4°C PBS and incubated with β-galactosidase staining solution (Sigma) at 37°C over night. Next day, embryos were photographed under a DMIL stereomicroscope (Leica). Sections (10 µm) of frozen embryos (*Stab2*-Cre;R26LacZ and *Lyve1*-Cre;R26LacZ) were fixed with 96% ethanol and pretreated with PBS containing 0.1% Triton-X100. After incubation in β-galactosidase reporter assay mix (Sigma) at 37°C over night sections were counterstained with Nuclear Fast Red (Sigma), mounted (Dako), and photographed with bright field microscope (Nikon).

Apoptosis assays. Embryo sections (2 µm) were stained for cleaved Caspase-3 and were used for TUNEL assay according to the manufacturer's protocol (Merck Millipore).

Western blot and ELISA. Western blotting was carried out as previously described (12). Luminescence signals were obtained with Luminata Forte Western HRP Substrate (Millipore) and detected by ChemoCam Imager (Intas Science Imaging). HUVEC cell culture supernatants were analysed with Human BMP2 DuoSet Elisa kit (R&D Systems).

Statistics. Statistical analysis was performed with SigmaPlot 11.0 Software (Systat Software). For comparisons, Student's t-test or one-way ANOVA were used, respectively. Differences between data sets with $p < 0.05$ were considered statistically significant. Data are presented as means with error bars indicating standard deviation.

Electron microscopy. Embryonic murine livers were dissected from E11.5 embryos and immediately immersed in fresh fixative for epoxy-embedding according to standard procedures. In brief, aldehyde fixation (2% formaldehyde, 2% glutaraldehyde, 0.5% tannic acid, 1 mM $MgCl_2$, 2% sucrose in 100 mM Na-cacodylate, pH 7.2), was followed by post-fixation in buffered 1% osmium tetroxide, dehydration, and resin-embedding. Ultrathin sections (60 nm) were contrast-stained with lead-citrate/uranylacetate and observed in a Zeiss EM 910 at 100 kV (Carl Zeiss). Micrographs were taken with image-plates, scanned at 30 µm resolution (Ditabis).

FACS. For flow cytometric analysis, E11.25 or E13.25 embryos were removed from the uterus and washed in HBSS/10% FCS. Yolk sacs (YS) were harvested and digested in HBSS/10% FCS containing collagenase IV (60 U/ml f.c., Sigma) and DNase I (25 µg/ml f.c., Sigma) for 1 h at 37°C. Fetal livers were harvested, mechanically dissociated and passed through a 100 µm cell strainer (BD). Embryos were exsanguinated into defined volumes of HBSS/10% FCS and blood samples were washed twice with PBS/5% FCS. Single cell suspensions were washed with PBS/5% FCS and Fc receptors were blocked by incubating cells with purified mouse IgG (500 mg/ml, Jackson ImmunoResearch Laboratories). All stainings were performed in PBS with 5% FCS on ice for 30 min with optimal dilutions of commercially-prepared antibodies. Reagents used were CD3e phycoerythrin (PE) (clone 145-C11, #12-0031-80), CD11b PerCP-Cy5.5 (clone M1/70, #45-0112-80), CD16/32 PE-Cy7 (clone 93, #25-0161-81), CD34 eFluor660 (RAM34, #50-0341-80), CD45 PE-Cy7 (clone 30-F11), CD45APC-eFlour780 (clone 30-F11, #47-0451-80), CD48 APC (clone HM 48-1, # 17-0481-80), CD117 A700 (ACK-2, #56-1172-80), F4/80 APC (clone BM8, # 17-4801-80), Sca-1 PerCP-Cy5.5 (clone D7, #45-5981-80), Ter119 PE-Cy7 (Ter119, # 25-5921-81) (all eBioscience), CD4 PE (H129.19, # 553652), CD8 PE (53-6.7, #553032), CD19 PE (clone 1D3, #553786), Gr-1 PE (clone RB6-8C5, # 561084), Ter119 PE (clone Ter119, # 553673), streptavidin APC-Alexa750 (#565144) (all BD) CD150 BV605 (clone TC15-12F12.2, #115927, Biolegend), streptavidin Qdot605 (#Q10001MP, Invitrogen). Stainings for apoptosis detection were performed using Annexin V Fitc apoptosis detection kit (BD) according to manufacturer's instruction. Cells were analysed on a FACS Fortessa (BD) and data were analysed using FACS Diva software (BD).

CFU assay determining the number of HSPCs. Singularized fetal liver cell extracts were harvested in Iscove's modified Dulbecco's medium (Thermo Fisher Scientific) containing 2% FCS (Biochrom) plated in gridded 35-mm-diameter cell culture dishes (Sarstedt) at concentrations of 5000 cells ml^{-1} per dish in triplicates. MethoCult™ mix #3434 (Stemcell Technologies) containing murine SCF, IL3, human IL6, human EPO, human insulin and human transferrin was used to stimulate mouse hematopoietic progenitor cells. Colonies were analysed after 7 and after 9 days with a Axio Vert.A1 microscope (Zeiss).

Fetal haemoglobin. Blood was taken from E11.5 and E14.5 embryos with a heparinized micro capillary. Relative haemoglobin values were analysed based on photometric detection of cyanmetahemoglobin.

Controls. For photomicrographs of the embryo, fetal organ dissection, immunofluorescence, immunohistochemistry, FACS analysis, CFU assays, electron microscopy, and determination of the fetal haemoglobin, cre-transgenic and cre-negativ siblings (e.g. *Stab2*-Cre$^{tg/wt}$;*Gata4*$^{fl/fl}$ versus *Stab2*-Cre$^{wt/wt}$;*Gata4*$^{fl/fl}$ and *Stab2*-Cre$^{wt/wt}$;*Gata4*$^{fl/wt}$) were compared. For transplantation and microarray analysis of the fetal liver *Stab2*-Cre$^{tg/wt}$;*Gata4*$^{fl/wt}$ animals were designated as controls.

References:

1. Shimshek DR, Kim J, Hubner MR, Spergel DJ, Buchholz F, Casanova E, Stewart AF, Seeburg PH, and Sprengel R. Codon-improved Cre recombinase (iCre) expression in the mouse. *Genesis.* 2002;32(1):19-26.
2. Lee EC, Yu D, Martinez de Velasco J, Tessarollo L, Swing DA, Court DL, Jenkins NA, and Copeland NG. A highly efficient Escherichia coli-based chromosome engineering system

adapted for recombinogenic targeting and subcloning of BAC DNA. *Genomics.* 2001;73(1):56-65.
3. Soriano P. Generalized lacZ expression with the ROSA26 Cre reporter strain. *Nature genetics.* 1999;21(1):70-1.
4. Srinivas S, Watanabe T, Lin CS, William CM, Tanabe Y, Jessell TM, and Costantini F. Cre reporter strains produced by targeted insertion of EYFP and ECFP into the ROSA26 locus. *BMC developmental biology.* 2001;1(4.
5. Pham TH, Baluk P, Xu Y, Grigorova I, Bankovich AJ, Pappu R, Coughlin SR, McDonald DM, Schwab SR, and Cyster JG. Lymphatic endothelial cell sphingosine kinase activity is required for lymphocyte egress and lymphatic patterning. *J Exp Med.* 2010;207(1):17-27.
6. Watt AJ, Battle MA, Li J, and Duncan SA. GATA4 is essential for formation of the proepicardium and regulates cardiogenesis. *Proc Natl Acad Sci U S A.* 2004;101(34):12573-8.
7. Wang J, Greene SB, Bonilla-Claudio M, Tao Y, Zhang J, Bai Y, Huang Z, Black BL, Wang F, and Martin JF. Bmp signaling regulates myocardial differentiation from cardiac progenitors through a MicroRNA-mediated mechanism. *Dev Cell.* 2010;19(6):903-12.
8. Kazanskaya O, Ohkawara B, Heroult M, Wu W, Maltry N, Augustin HG, and Niehrs C. The Wnt signaling regulator R-spondin 3 promotes angioblast and vascular development. *Development.* 2008;135(22):3655-64.
9. Augustin I, Goidts V, Bongers A, Kerr G, Vollert G, Radlwimmer B, Hartmann C, Herold-Mende C, Reifenberger G, von Deimling A, et al. The Wnt secretion protein Evi/Gpr177 promotes glioma tumourigenesis. *EMBO Mol Med.* 2011;4(1):38-51.
10. Phaneuf D, Moscioni AD, LeClair C, Raper SE, and Wilson JM. Generation of a mouse expressing a conditional knockout of the hepatocyte growth factor gene: demonstration of impaired liver regeneration. *DNA and cell biology.* 2004;23(9):592-603.
11. Waskow C, Madan V, Bartels S, Costa C, Blasig R, and Rodewald HR. Hematopoietic stem cell transplantation without irradiation. *Nature methods.* 2009;6(4):267-9.
12. Klein D, Demory A, Peyre F, Kroll J, Augustin HG, Helfrich W, Kzhyshkowska J, Schledzewski K, Arnold B, and Goerdt S. Wnt2 acts as a cell type-specific, autocrine growth factor in rat hepatic sinusoidal endothelial cells cross-stimulating the VEGF pathway. *Hepatology.* 2008;47(3):1018-31.
13. Diehl L, Schurich A, Grochtmann R, Hegenbarth S, Chen L, and Knolle PA. Tolerogenic maturation of liver sinusoidal endothelial cells promotes B7-homolog 1-dependent CD8+ T cell tolerance. *Hepatology.* 2008;47(1):296-305.
14. Viemann D, Schmidt M, Tenbrock K, Schmid S, Muller V, Klimmek K, Ludwig S, Roth J, and Goebeler M. The contact allergen nickel triggers a unique inflammatory and proangiogenic gene expression pattern via activation of NF-kappaB and hypoxia-inducible factor-1alpha. *Journal of immunology.* 2007;178(5):3198-207.
15. Mostoslavsky G, Fabian AJ, Rooney S, Alt FW, and Mulligan RC. Complete correction of murine Artemis immunodeficiency by lentiviral vector-mediated gene transfer. *Proc Natl Acad Sci U S A.* 2006;103(44):16406-11.
16. Evdokimov K, Biswas S, Adrian M, Weber J, Schledzewski K, Winkler M, Goerdt S, and Geraud C. Proteolytic cleavage of LEDA-1/PIANP by furin-like proprotein convertases precedes its plasma membrane localization. *Biochemical and biophysical research communications.* 2013;434(1):22-7.
17. Schledzewski K, Geraud C, Arnold B, Wang S, Grone HJ, Kempf T, Wollert KC, Straub BK, Schirmacher P, Demory A, et al. Deficiency of liver sinusoidal scavenger receptors stabilin-1 and -2 in mice causes glomerulofibrotic nephropathy via impaired hepatic clearance of noxious blood factors. *J Clin Invest.* 2011;121(2):703-14.

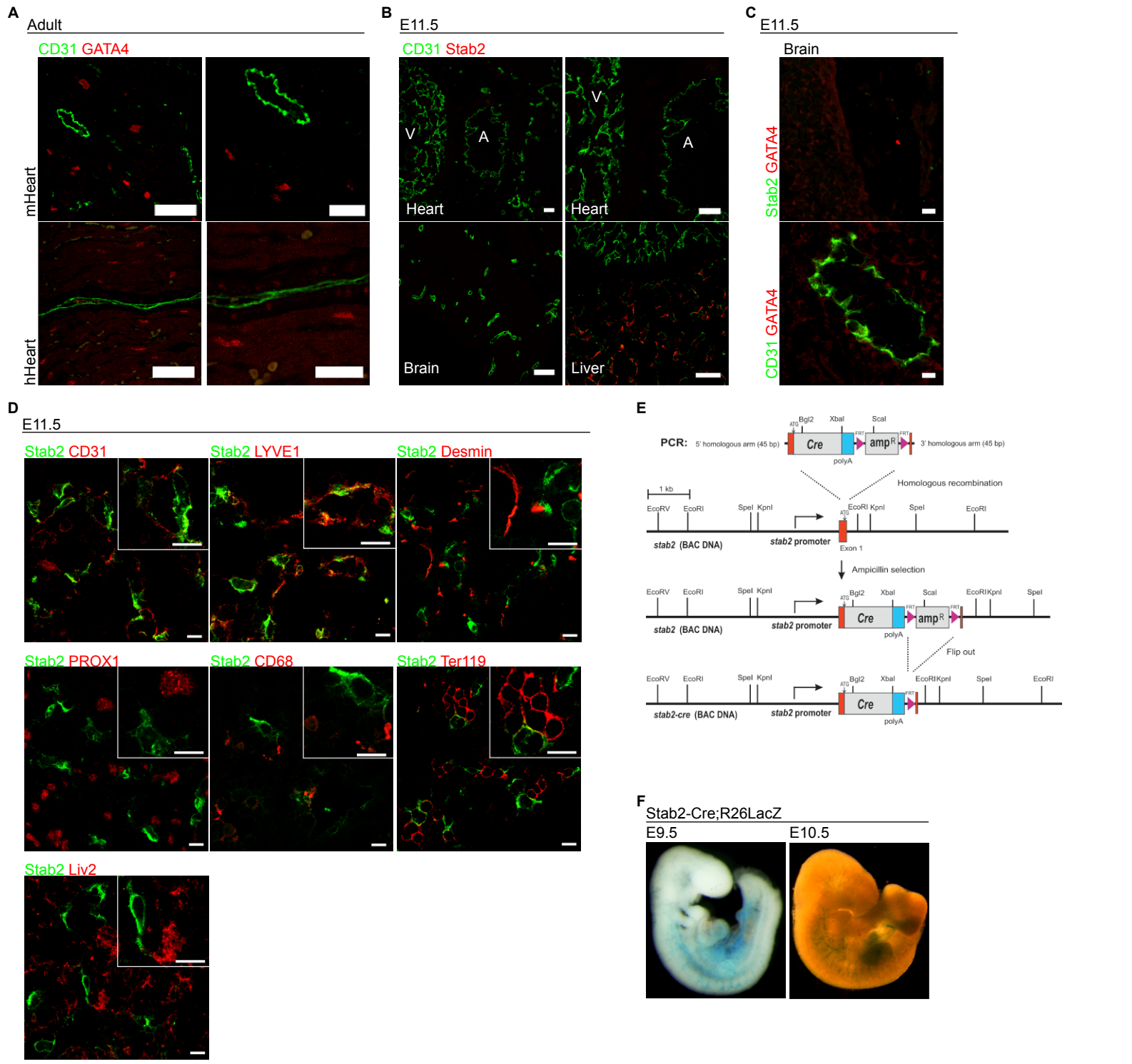

G

	E10.5 - E15.5	E17.5	P0
Stab2-Cre$^{wt/wt}$;Gata4$^{fl/wt}$	191 (25.4 %)	2 (18.2 %)	50 (33.5 %)
Stab2-Cre$^{wt/wt}$;Gata4$^{fl/fl}$	176 (23.4 %)	3 (27.3 %)	56 (37.5 %)
Stab2-Cre$^{tg/wt}$;Gata4$^{fl/wt}$	188 (25.0 %)	4 (36.4 %)	43 (29.0 %)
Stab2-Cre$^{tg/wt}$;Gata4$^{fl/fl}$	196 (26.1 %)	0*	0

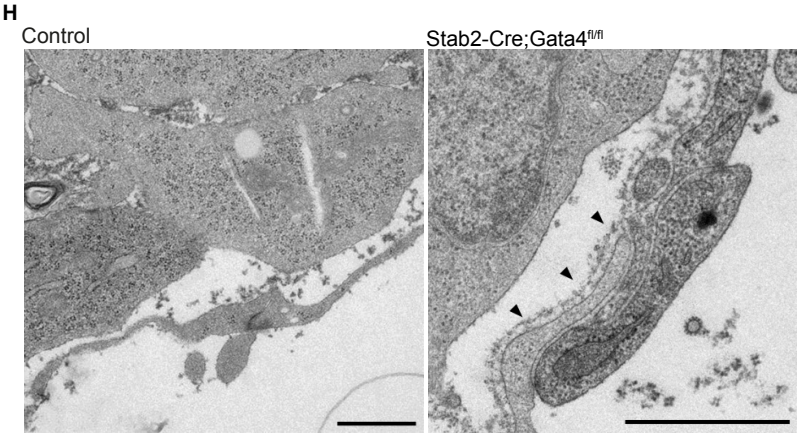

Supplementary Figure 1. Endothelial expression of GATA4 and Stab2, and generation and characterization of *Stab2-Cre*;R26LacZ and *Stab2-Cre;Gata4*$^{fl/fl}$ mice. (**A**) Co-IF shows absence of GATA4$^+$ nuclei in CD31$^+$ endothelium of adult human (hHeart) and mouse (mHeart) heart (n = 3). Scale bar 60 µm (left panel) and 25 µm (right panel). (**B**) Co-IF of Stab2 with CD31 in the cardiac atrium (A) and ventricle (V), the brain and the liver of wildtype embryos at E11.5 (n = 3). Scale bar 50 µm. (**C**) Co-IF of GATA4 with Stab2 and CD31 in the brain of wildtype embryos at E11.5 (n > 3). Scale bar 10 µm. (**D**) Co-IF of Stab2 with CD31, LYVE1, Desmin, Liv2, PROX1, CD68, and Ter119 in the liver of wildtype embryos at E11.5 (n = 3). Scale bar 10 µm. (**E**) Generation of the *Stab2-Cre* transgenic construct. Amplification of *cre* cDNA by PCR and insertion into exon 1 of *stab2* on bacmid RPCIB731O23129Q by homologous recombination in *E. coli*. Ampicillin selection of positive clones and Flip-mediated recombination of the ampicillin cassette. (**F**) Whole mount β-galactosidase staining of *Stab2-Cre*;R26LacZ embryos at E9.5 and E10.5 shows major reporter activity in the fetal liver (n = 5). (**G**) Survival rate of embryonic and adult *Stab2-Cre;Gata4* mice. Normal Mendelian ratio from E10.5 to E15.5, no living *Stab2-Cre;Gata4*$^{fl/fl}$ mice were detected at E17.5 and P0 (asterisk: 2 *Stab2-Cre;Gata4*$^{fl/fl}$ embryos at E17.5 were found deceased in utero). (**H**) TEM of the liver of *Stab2-Cre;Gata4*$^{fl/fl}$ embryos at E11.5. Arrowheads indicate formation of a basement membrane (n = 4). Scale bar 1 µm.

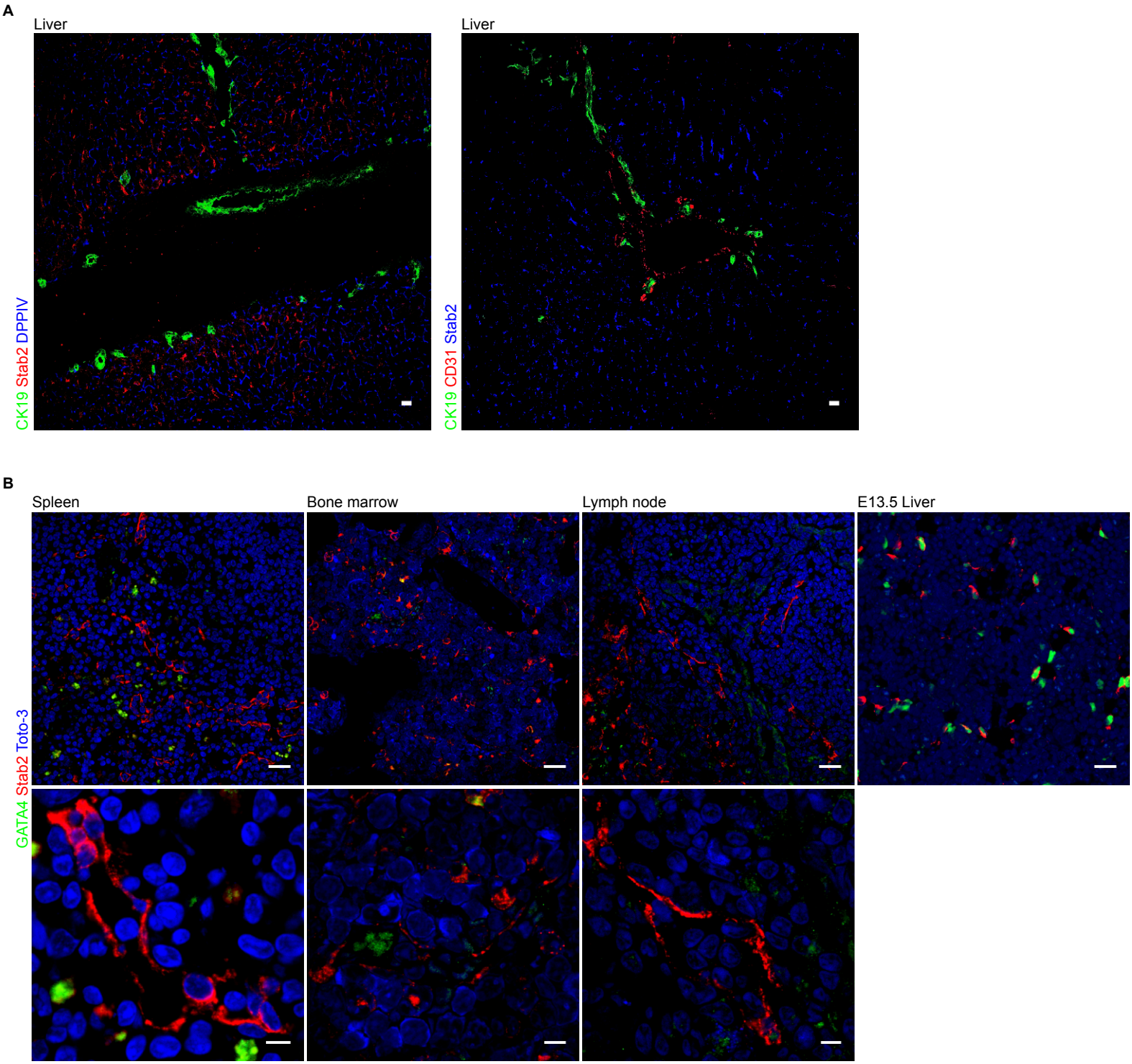

Supplementary Figure 2. Analysis of Stab2 in adult liver and GATA4 in adult spleen, bone marrow, and lymph node. (**A**) Co-IF of Stab2, CK19, and DPPIV in adult murine liver (n = 5). Scale bar 20 µm. (**B**) Co-IF of GATA4 and Stab2 in adult murine spleen, bone marrow, and lymph node. Fetal liver from E13.5 mice serves a positive control (n = 3). Scale bar 20 µm (upper panel) and 5 µm (lower panel).

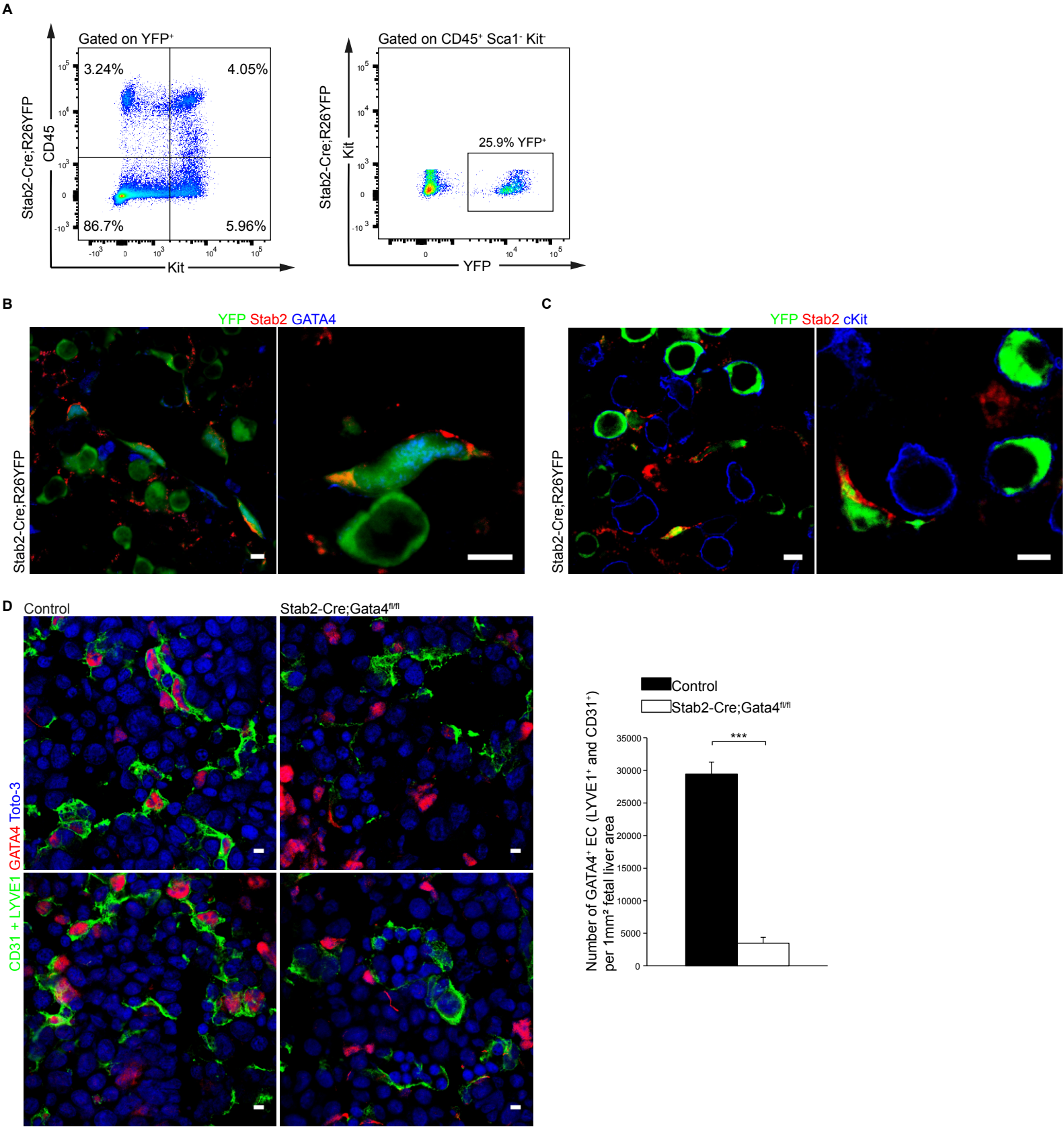

Supplementary Figure 3. Characterization of *Stab2-Cre*;R26YFP mice and GATA4 knockdown efficiency in *Stab2-Cre;Gata4*$^{fl/fl}$ LSEC. (**A**) FACS analysis of fetal liver cells of *Stab2-Cre*;R26YFP reporter mice at E13.25. Representative FACS blots show CD45 and Kit expression in YFP$^+$ cells (left panel) and YFP reporter activity in CD45$^+$Sca1$^-$Kit$^-$ cells (right panel) (n = 5). (**B**) Co-IF of YFP, Stab2, and GATA4 in *Stab2-Cre*;R26YFP embryos at E12.5 (n = 3). Scale bar 5 µm. (**C**) Co-IF of YFP, Stab2, and cKit in *Stab2-Cre*;R26YFP embryos at E12.5 (n = 3). Scale bar 5 µm. (**D**) Co-IF of GATA4, CD31, LYVE1, and Toto-3 in *Stab2-Cre;Gata4*$^{fl/fl}$ embryos at E11.5 (left panel). Scale bar 5 µm. Quantification of GATA4-positive EC (CD31$^+$ and/or LYVE1$^+$) (right panel) (n = 4). Student's *t* test: ***$p < 0.001$.

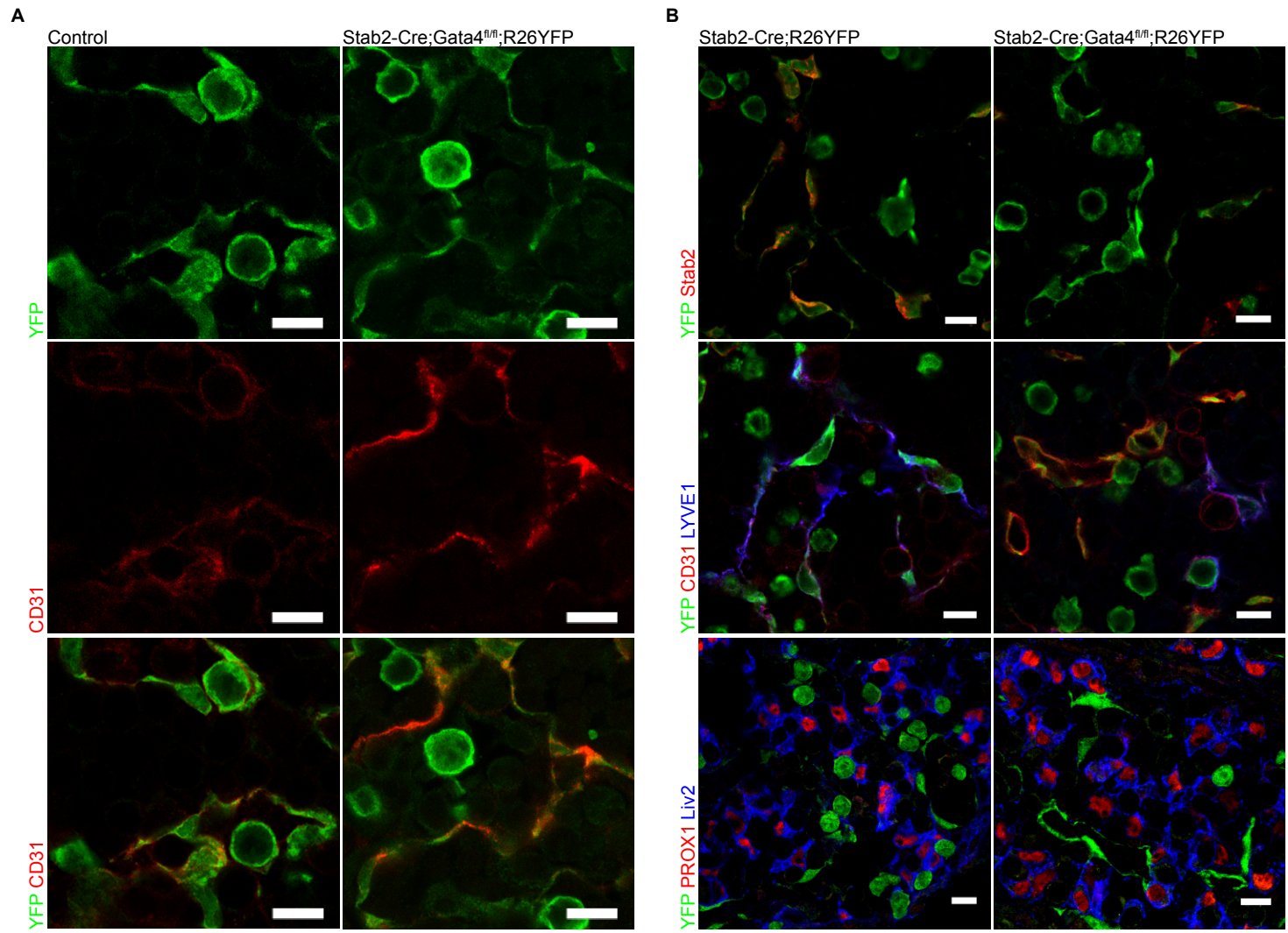

Supplementary Figure 4. The capillarized micro-vasculature in the fetal liver of *Stab2-Cre;Gata4*;R26YFP mutant mice is composed of GATA4-deficient, transgenic EC. (**A**) Co-IF shows an increased expression of CD31 in YFP$^+$ transgenic endothelium in the liver of *Stab2-Cre;Gata4*$^{fl/fl}$;R26YFP embryos at E11.5 (n = 3). Scale bar 10 µm. (**B**) Co-IF of YFP and Stab2, CD31, LYVE1, PROX1, or Liv2 in the liver of *Stab2-Cre*;R26YFP and *Stab2-Cre;Gata4*$^{fl/fl}$;R26YFP embryos at E11.5 (n = 4). Scale bar 10 µm.

A

E13.5

Lyve1-Cre;R26LacZ

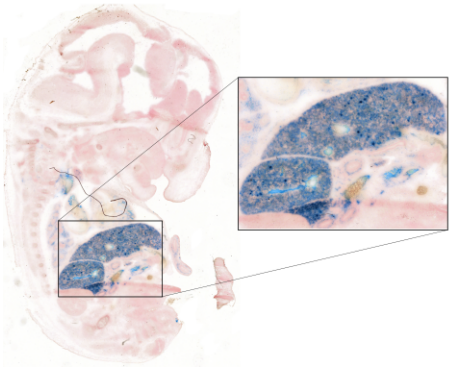

B

Lyve1-Cre;R26YFP

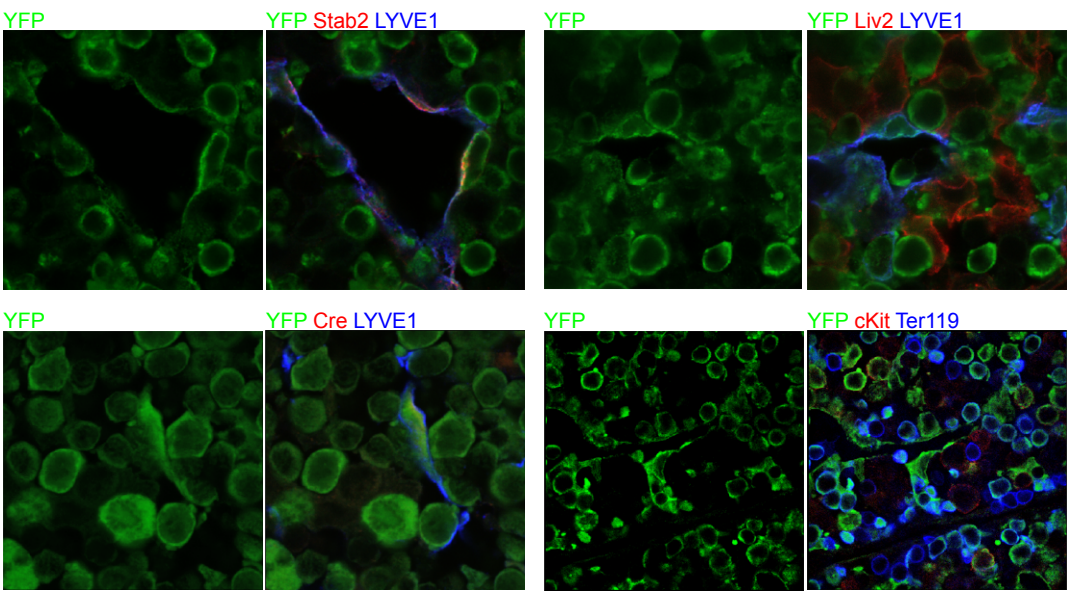

C

	E11.5 - E14.5	P0
Lyve1-Cre$^{wt/wt}$;Gata4$^{fl/wt}$	19 (24.4 %)	17 (35.4 %)
Lyve1-Cre$^{wt/wt}$;Gata4$^{fl/fl}$	18 (23.1 %)	17 (35.4 %)
Lyve1-Cre$^{tg/wt}$;Gata4$^{fl/wt}$	23 (29.5 %)	14 (29.2 %)
Lyve1-Cre$^{tg/wt}$;Gata4$^{fl/fl}$	18 (23.1 %)	0

D

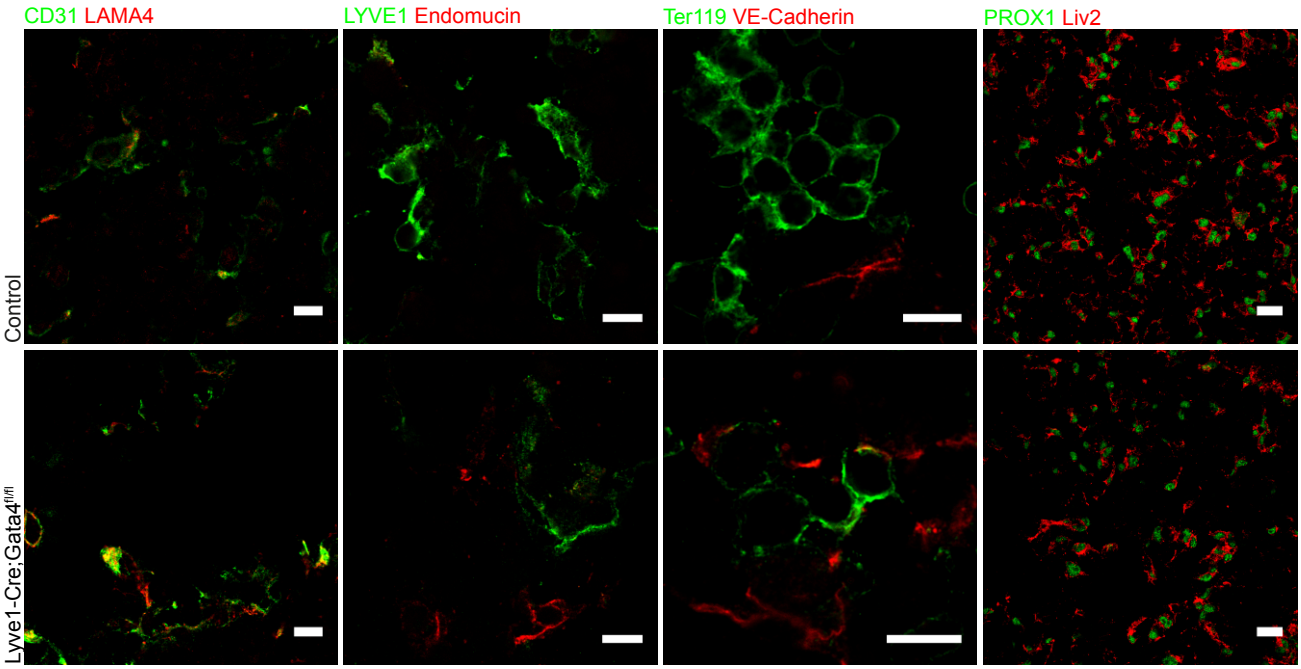

Supplementary Figure 5. Lyve1-Cre mice: reporter analysis and GATA4 deletion in LSEC. (**A**) Analysis of Lyve1-Cre;R26LacZ (β-galactosidase assay) mouse shows reporter activity in the endothelium of the liver at E13.5 (n = 3). (**B**) Co-IF of YFP with Stab2, LYVE1, Liv2, Cre, cKit, and Ter119 in the fetal liver of Lyve1-Cre;R26YFP reporter mice at E12.5 (n = 3). (**C**) Survival rate of adult and embryonic *Lyve1-Cre;Gata4* mice. Normal Mendelian ratio from E11.5 to E14.5, no living *Lyve1-Cre;Gata4*$^{fl/fl}$ mice were detected at P0. (**D**) Co-IF of CD31 and LAMA4, LYVE1 and Endomucin, PROX1 and Liv2, and VE-Cadherin and Ter119 in the liver of *Lyve1-Cre;Gata4*$^{fl/fl}$ embryos at E11.5 (n = 2). Scale bar 10 µm and 20 µm (last panel).

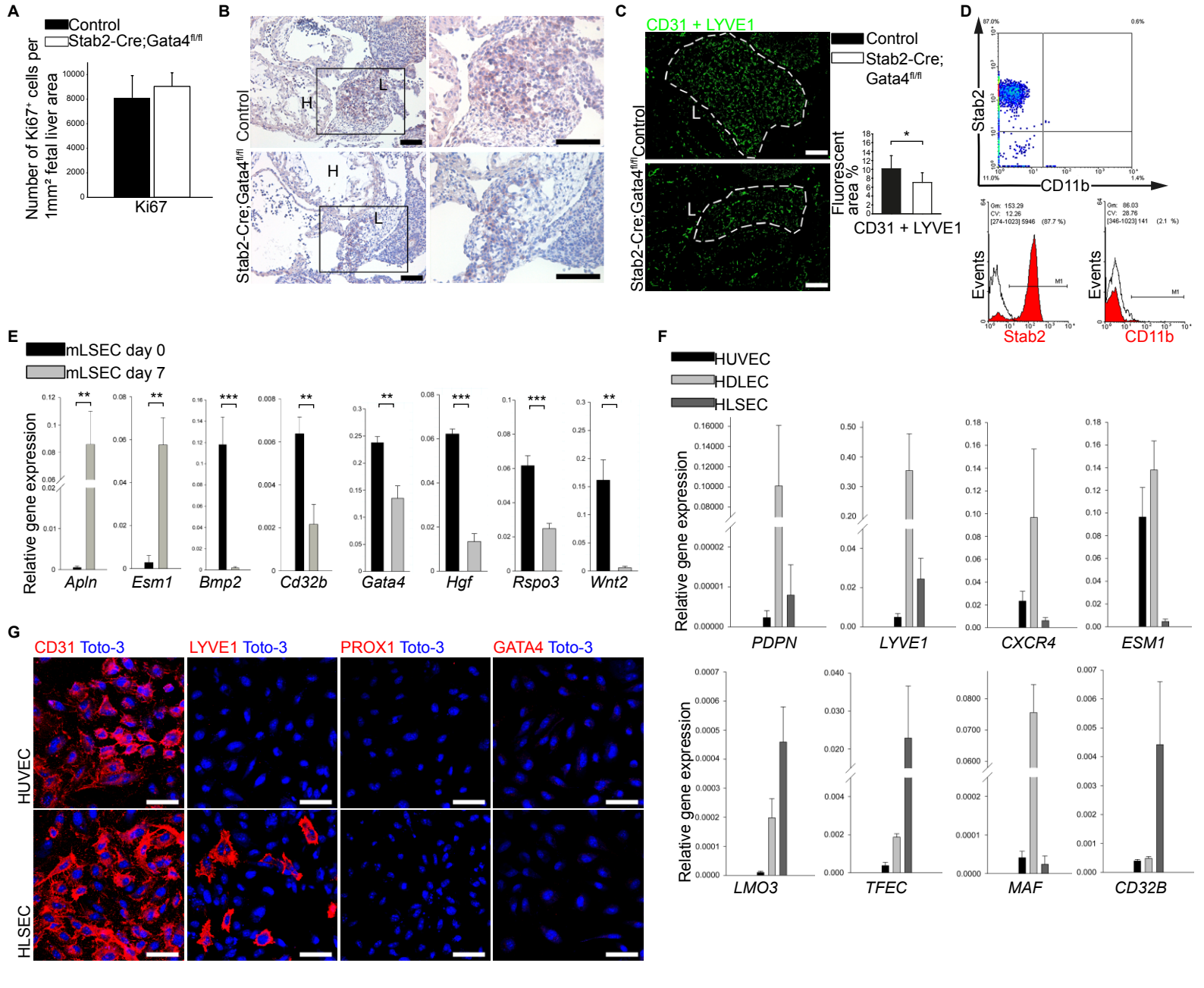

Supplementary Figure 6. Proliferation and oxygen supply in the liver of *Stab2-Cre;Gata4*$^{fl/fl}$ embryos, and characterization of primary mouse LSEC and of primary human EC cell lines transduced by Gata4. (**A**) Proliferation rate of liver cells of *Stab2-Cre;Gata4*$^{fl/fl}$ embryos at E11.5. Quantification based on IF of Ki67 (n = 2). (**B**) Oxygen supply was examined by IHC with Hypoxyprobe ™ (anti-Pimonidazol) in the liver of *Stab2-Cre;Gata4*$^{fl/fl}$ embryos at E10.5 (n = 3). Scale bar 20 µm. (**C**) Overlay from IF of CD31 and LYVE1 in the liver of *Stab2-Cre;Gata4*$^{fl/fl}$ embryos at E11.5 and quantification of the respective fluorescent area (n = 3). Scale bar 250 µm. (**D**) Purity of isolated mLSECs by FACS analysis using Stab2 (LSEC) and CD11b (macrophages/Kupffer cells) antibodies. (**E**) Murine LSEC rapidly dedifferentiate in culture. QRT-PCR of cDNA derived from mLSEC freshly isolated (day 0) or mLSEC kept in culture for seven days (day 7) show expression levels of endothelial genes *Apln*, *Esm1*, *Bmp2*, *Cd32b*, *Gata4*, *Hgf*, *Rspo3*, and *Wnt2* (n > 3). (**F**) Expression levels of endothelial genes *CD32B*, *PDPN*, *LYVE1*, *CXCR4*, *ESM1*, *LMO3*, *TFEC*, and *MAF* by qRT-PCR of cDNA derived from HUVEC, HLSEC (human LSEC), and HDLEC (human dermal lymphatic EC) (n = 3). (**G**) LSEC-associated and lymphatic endothelial cell-associated transcription factors GATA4 and PROX1, respectively, were not expressed in HUVEC or HLSEC. Co-IF of CD31, PROX1, LYVE1, and GATA4 in HUVEC and HLSEC (n = 3). Scale bar 50 µm. (**H**) Transduction of HUVEC and HLSEC by Gata4. Co-IF and WB of *GATA4*-transduced HUVEC and HLSEC either co-stained for GATA4 and Phalloidin (upper panel) or probed with anti-GATA4, anti-β-Actin and anti-Gapdh antibodies (lower panel) (n = 3). Scale bar 60 µm. Student's *t* test: **p* < 0.05; ***p* < 0.01; ****p* < 0.001.

Cluster	Downregulated genes in Stab2-Cre;Gata4fl/fl fetal liver				number of genes shown to bind Gata4 in liver ChIP-seq	Upregulated genes in Stab2-Cre;Gata4$^{fl/fl}$ fetal liver				number of genes shown to bind Gata4 in liver ChIP-seq
Liver sinusoidal endothelial	Aqp1 Ehd3 Fcna	Gpr182 Kcnk6 Lyve1	Mrc1 Slc40a1	Stab2	8/9					0/0
Endothelial/ non-LSEC	Ear2	Kcnk6	Tnfrsf14	Tspo	2/4	8430408G22Rik Adm2 Cav1 Col15a1 Efna1 Emcn Epha4 Fgfr1	Flrt3 Gabre Gja1 Has2 Hey1 Hk2 Kcnj8 Lama4	Meox2 Mfap4 Ntrk3 Pfkfb3 Pfn2 Plxdc2 Rgs4 Rgs5	Rps6ka2 Snai2/Slug Sparcl1 Stc1 Vcan Vegfa Vldlr	11/31
Pericytes					0/0	Mfap4	Pdgfra	Plxdc2	RGS5	1/4
Hematopoietic/ myeloid	AB124611 Abcg3 Ache AI662270 Alox5ap C1qb C1qc Cd180 Cd52 Cd53 Cd5l Cd86 Cfp Clec4a1 Clec4a3	Clec5a Clec7a Cpa3 Csf1r Ctss Ear2 Emr1 Emr4 Fcna Folr2 Fyb Ms4a3 Hdc Hmox1 Ifi47	Igsf6 Il6ra Kcnk6 Marco Mpeg1 Mpo Mrc1 Ms4a6d Nr1h3 P2ry13 P2ry6 Pkhd1l1 Pld4 Ptprc S100a9	Slamf1 Slc11a1 Spi1 Spic Stfa2l1 Tbxas1 Tfec Themis2 Timd4 Tnfrsf14 Treml1 Treml4 Tspo Tyrobp Unc93b1	6/60	Akr1c12				0/1
Hematopoietic/ erythrocytes	Ampd3 Cldn13 Folr2	Igsf6 Itgal Ms4a3	Rhd Slamf1	Spi1 Trim10	0/10	6330403K07Rik	Akr1c12			0/2
Parenchymal	Abcc3 Ctss Ear2	Nr1h3	Slc40a1	Uros	2/5	Bhlhe40 Cth Cyp39a1	Ddit4 Mir122a	Plod2 Slc38a3	Slc7a3 Trp53i11	2/9
Extracellular matrix	Fcna				0/1	Frem1	Prnd	Stc2		0/3
Neuronal	Snca				0/1	Fsd1 Gabre Glrb	Gpc6 Nkain1 Rcor	Rimklb Ror2	Snai2/Slug Ypel1	1/10
HIF/Hypoxia-associated					0/0	Aldoc Ankrd37 Dact1 Ddit4 Efna1	Egln3 Fgf11 Gys1 Hey1 Hk2	Ndufa4l2 Pfkfb3 Plod2 Rgs4 Rps6ka	Stc1 Stc2 Vegfa Vldlr	4/19
Apoptosis-associated	Cd53 Ear2	Fcna Gpr65	Plac8 Spi1	Timd4	0/7	Bhlhe40 Clip3	Hk2 Prnd	Rnf122	Tox3	1/6
Ubiquitous	2610305D13Rik A730089K16Rik Atp8b4 Cisd3 Cyth4	D030028A08Rik Emc9 Fam117a Glipr1 Hebp1	Hmga2-ps1 Mc2r Naip6 Nxpe2 Plac8	Rgcc Slc22a3 Slc46a3 Slc6a4 Tspan8	3/20	A330076H08Rik B130024G19Rik Fam155a Fgf11	Gm129 Gys1 Hist1h2bg Kcne3	Nfib Nr1h5 Pgm5	Rab2b Tmem255a	1/14

Supplementary Figure 7. Gene expression profiling of the fetal liver from *Stab2-Cre;Gata4*$^{fl/fl}$ embryos at E11.5. Upon gene expression profiling with Affymetrix cDNA-microarrays, 98 genes were significantly down-regulated (light blue) and 80 genes were significantly up-regulated (light red) with a fold change of ≤ -2 or ≥ 2 in the mutant liver. The differentially expressed genes were grouped into one (or two) clusters referring to cellular expression by systematic database searches. Genes that have been shown to interact with transcription factor GATA4 in a ChIP-seq analysis of adult murine liver [Zheng et al., 2013] were underlined. Frequency of these GATA4 target genes within the clusters are further visualized as bar chart (black) (n = 3).

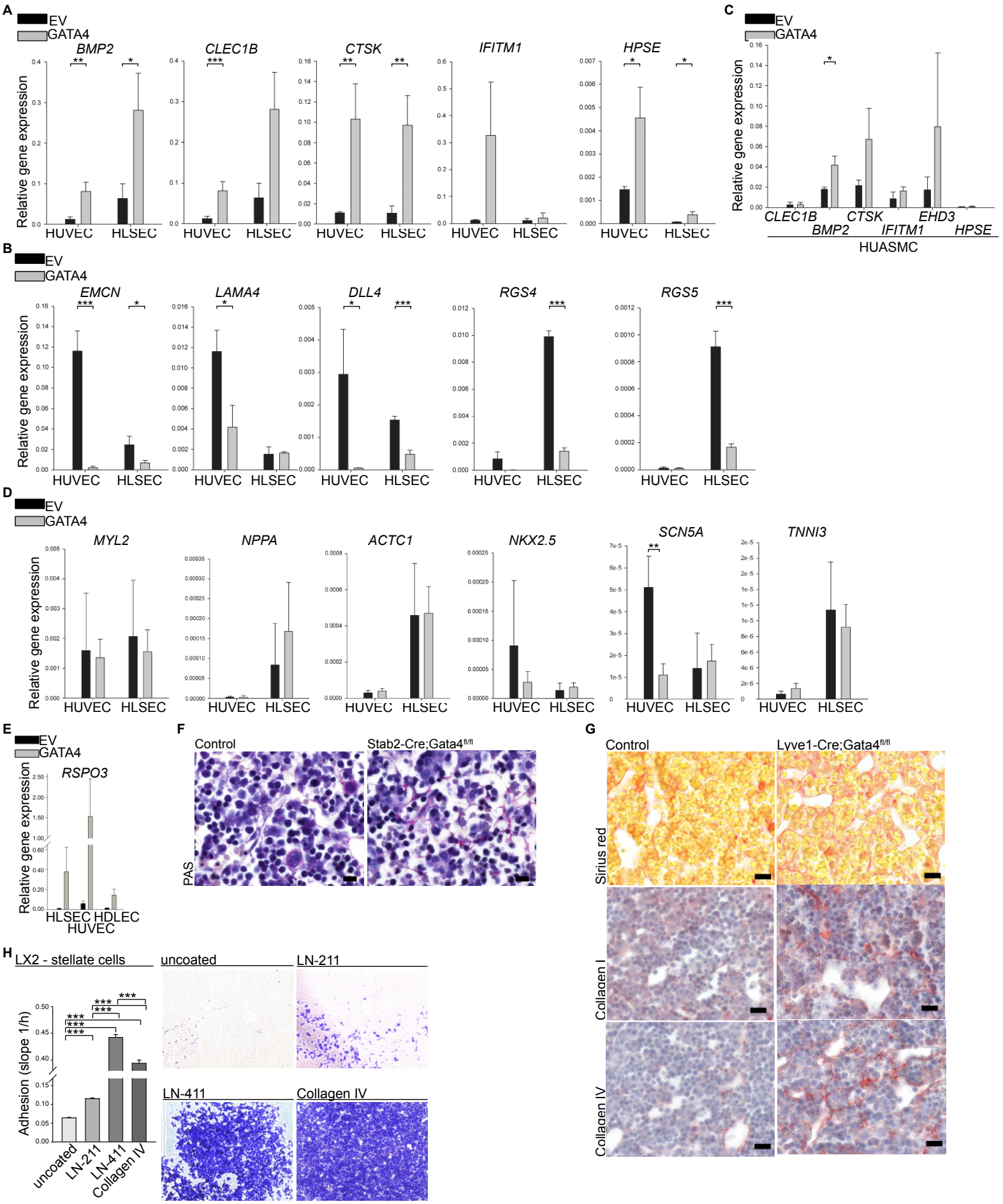

Supplementary Figure 8. GATA4-mediated gene regulation is context-dependent and characterization of the extracellular matrix in *Stab2-Cre;Gata4*$^{fl/fl}$ embryos. (**A**-**B**) Regulation of LSEC-associated and continuous EC-associated genes by GATA4 in human endothelial cell lines in vitro. QRT-PCR of *GATA4*-transduced HUVEC and HLSEC. LSEC-associated genes are up-regulated (**A**) whereas genes expressed by continuous EC are down-regulated (**B**) by GATA4 (n > 3). (**C**) Regulation of GATA4- dependent endothelial-associated genes does only occur in an endothelial cell context. QRT-PCR of *GATA4*-transduced HUASMC (Human Umbilical Artery Smooth Muscle Cells). Except for *BMP2*, no significant GATA4-dependent regulation of endothelial genes was shown in HUASMC (n > 3). (**D**) Regulation of GATA4-dependent cardiomyocyte-associated genes does not occur in an endothelial cell context. QRT-PCR of *GATA4*-transduced HUVEC and HLSEC. Known GATA4-dependent, cardiomyocyte-associated genes were not significantly regulated by GATA4 in endothelial cell lines (n > 3). (**E**) Regulation of *RSPO3* by GATA4 in human endothelial cell lines in vitro. QRT-PCR of *GATA4*-transduced HUVEC, HLSEC and HDLEC (n > 3). (**F**) Periodic acid–Schiff (PAS) staining in the liver of *Stab2-Cre;Gata4*$^{fl/fl}$ embryos at E13.5 (n = 3). Scale bars 10 µm. (**G**) Sirius red staining (left panel) and IHC of Collagen I and Collagen IV in the fetal liver of *Lyve1-Cre;-Gata4*$^{fl/fl}$ embryos at E13.5 (n = 4). Scale bars 20 µm. Student's *t* test: *$p < 0.05$; **$p < 0.01$; ***$p < 0.001$. (**H**) LX2 cell adhesion on Laminin-411 (LN-411), Collagen IV, and Laminin-211 (LN-211) measured by the xCELLigence system. Slope is representing the change of the cell index (n = 7). ANOVA: ***$p < 0.001$. Crystal violet staining of adherent LX2 cells on LN-411, Collagen IV, and LN-211 (n = 5).

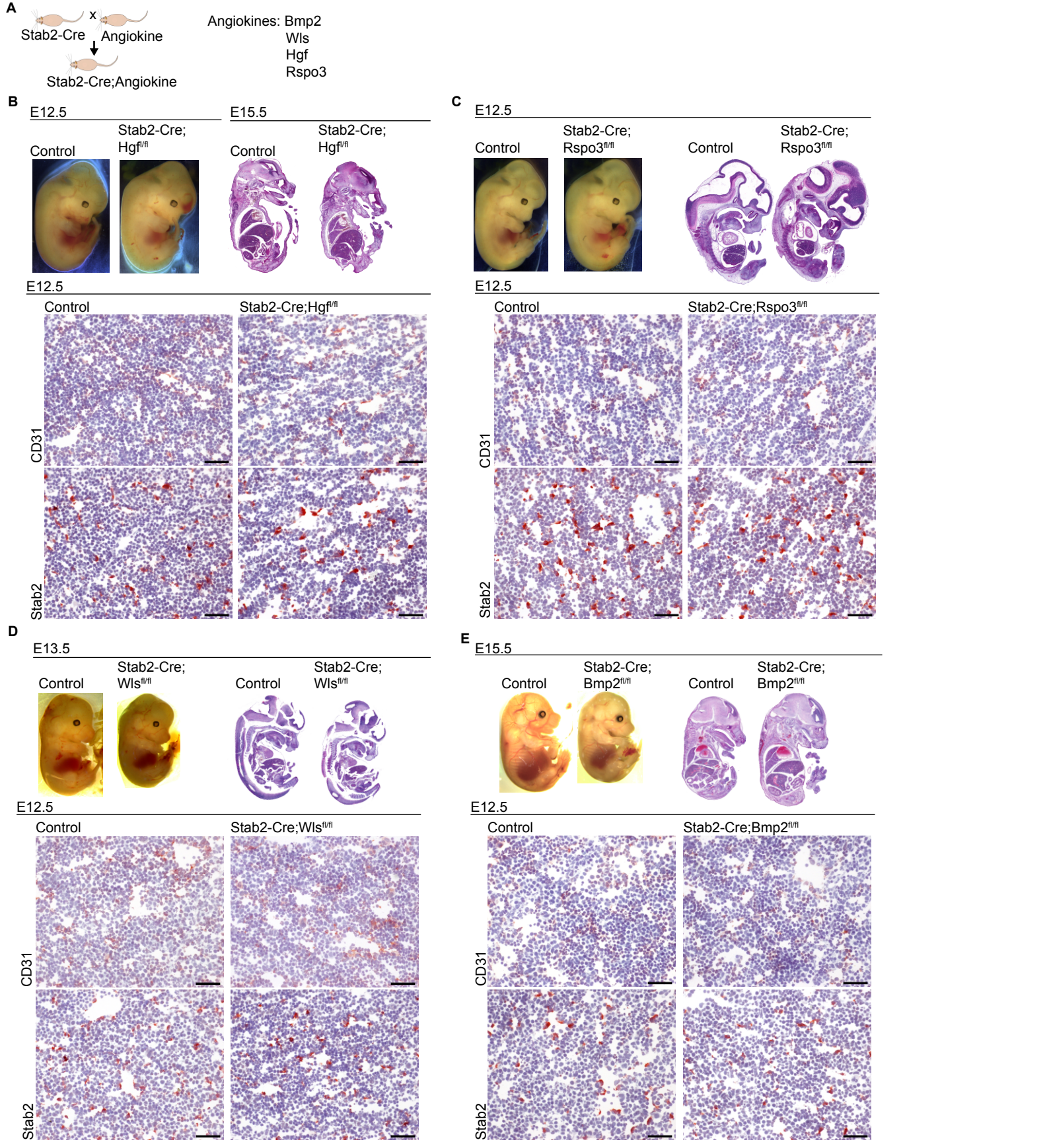

Supplementary Figure 9. *Stab2-Cre*-mediated deletion of LSEC-associated angiokines. (**A**) Floxed *Hgf*, *Rspo3*, *Wls* and *Bmp2* mice were crossed to *Stab2-Cre* mice resulting in *Stab2-Cre*;angiokine mice that are deficient in the respective angiokine. (**B**) *Stab2-Cre*;Hgf$^{fl/fl}$ embryos did not show overall phenotypical abnormalities or a hypoplastic liver at E12.5. H&E staining confirmed a normal liver and grossly normal other organs. No obvious differences of hepatic micro-vessels were observed upon loss of hepatic endothelial Hgf. Expression of continuous (CD31) as well as liver sinusoidal endothelial marker molecule (Stab2) remained unchanged in the mutant fetal liver (n = 3). Scale bar 50 µm. (**C**) *Stab2-Cre*;Rspo3$^{fl/fl}$ embryos did not show overall phenotypical abnormalities or a hypoplastic liver at E12.5. H&E staining confirmed a normal liver and grossly normal other organs. No obvious differences of hepatic micro-vessels were observed upon loss of hepatic endothelial RSPO3. Expression of CD31 as well as of Stab2 remained unchanged in the mutant fetal liver (n = 3). Scale bar 50 µm. (**D**) *Stab2-Cre*;Wls$^{fl/fl}$ embryos did not show overall phenotypical abnormalities or a hypoplastic liver at E13.5. H&E confirmed a normal liver and grossly normal other organs. No obvious differences of hepatic micro-vessels were observed upon loss of hepatic endothelial Wls. Expression of CD31 as well as of Stab2 remained unchanged in the mutant fetal liver (n = 3). Scale bar 50 µm. (**E**) *Stab2-Cre*;Bmp2$^{fl/fl}$ embryos did not show overall phenotypical abnormalities or a hypoplastic liver at E15.5. H&E staining confirmed a normal liver and grossly normal other organs. No obvious differences of hepatic micro-vessels were observed upon loss of hepatic endothelial BMP2. Expression of CD31 as well as of remained unchanged in the mutant fetal liver (n = 3). Scale bar 50 µm.

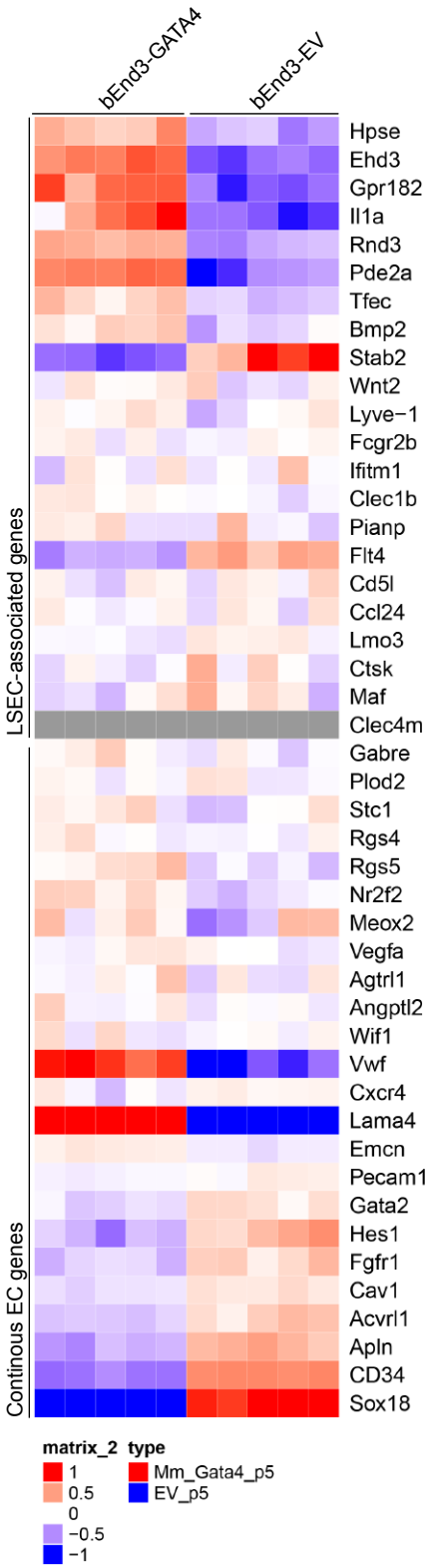

Supplementary Figure 10. Gene expression analysis of *GATA4*-transduced brain endothelial cells. Heatmap of LSEC-associated and continuous EC-associated genes comparing *GATA4*-transduced with EV-transduced brain endothelial cells (bEnd3).